Electronic Supplementary Information

Peptide Bond Formation by Aminolysin-*A* Catalysis: A Simple Approach to Enzymatic Synthesis of Diverse Short Oligopeptides and Biologically Active Puromycins

Hirokazu Usuki, Yukihiro Yamamoto, Jiro Arima, Masaki Iwabuchi, Shozo Miyoshi, Teruhiko Nitoda, and Tadashi Hatanaka*

E-mail: hatanaka@bio-ribs.com

Contents

Section-1. List of family S9 peptidases used for the construction of an unrooted dendrogram (Figure 1 of the main text).

Table S1. Family S9 enzymes from different species used for the construction of phylogenetic trees

Entry	Species	Domain of life	AccesionNO	Subfamily
1	*Leishmania major*	Eukarya	CAJ02700.1	S9A
2	*Trypanosoma cruzi*	Eukarya	EAN84486.1	S9A
3	*T. brucei*	Eukarya	EAN80234.1	S9A
4	*Mycobacterium leprae*	Bacteria	CAB08412	S9A
5	*M. tuberculosis H37Rv*	Bacteria	CAB02371	S9A
6	*M. lacunata*	Bacteria	BAA07460	S9A
7	*T. denticola*	Eukarya	AAK39550	S9A
8	*Estercia coli*	Bacteria	BAA01750	S9A
9	*Pyrococcus furiosus*	Archaea	AAA73423	S9A
10	*Streptomyces griseus*	bacteria	B1VWJ6	S9A
11	*Aeromonas hydrophila*	Bacteria	BAA03105	S9A
12	*Elizabethkingia meningoseptica*	Bacteria	BAA01755	S9A
13	*Sphingomonas capsulata*	Bacteria	BAA34052	S9A
14	*Arabidopsis thalian*	Eukaryota	NP_001117606	S9A
15	*Arabidopsis thalian*	Eukaryota	Q9LN30	S9A
16	Porcine	Eukaryota	AAA31110	S9A
17	*Arabidopsis thaliana*	Eukaryota	Q9FNF6	S9B
18	*Drosophila melanogaster*	Eukaryota	Q9VC19	S9B
19	Homo sapiens	Eukaryota	EAW77731	S9B
20	Homo sapiens	Eukaryota	EAW69199	S9B
21	*Porphyromonas gingivalis*	Bacteria	MER005196[1)]	S9B
22	*Pseudomonas sp. WO24*	Bacteria	BAD27580	S9B
23	*Chryseobacterium meningosepticum*	Bacteria	Q47900	S9B
24	*Aspergillus oryzae*	Eukaryota	O42812	S9B
25	*Saccharomyces cerevisiae*	Eukaryota	P18962	S9B
26	*Saccharomyces cerevisiae*	Eukaryota	P33894	S9B
27	Homo sapiens	Eukaryota	P27487	S9B
28	Homo sapiens	Eukaryota	Q12884	S9B
29	*Acidothermus cellulolyticus*	Bacteria	YP_873767	S9C
30	*Streptomyces avermitilis*	Bacteria	NP_825741	S9C
31	*Streptomyces coelicolor*	Bacteria	Q9XAJ2	S9C
32	*Arabidopsis thaliana*	Eukaryota	Q84LM4	S9C
33	*Oryza sativa*	Eukaryota	A3C4R4	S9C
34	*Oryza sativa*	Eukaryota	ABB47613	S9C
35	*Nematostella vectensis*	Eukaryota	EDO40564	S9C
36	Sus scrofa	Eukaryota	P19205	S9C
37	Homo sapiens	Eukaryota	P13798	S9C
S. morookaensis, PMH	*Streptomyces morookaensis*	Bacteria	BAE79346	unknown
S. coelicolor, AP	*S. coelicolor*	Bacteria	Q9ZBI6	unknown
S. griseus, AP	*S. griseus*	Bacteria	SGR1153[2)]	unknown
S. thermocyaneoviolaceus, AP	*S. thermocyaneoviolaceus*	Bacteria	AB480284	unknown
A. cellulolyticus, AP (This work)	*Acidothermus cellulolyticus*	Bacteria	YP_873247	unknown

1) ID of MEROPS data base (http://merops.sanger.ac.uk/), 2) ID of *Streptomyces griseus* genome project (http://streptomyces.nih.go.jp/griseus/)

Section-2: Enzymatic characteristics of wild type S9 ACAP

The purified enzyme was used for these experiments. The standard assays were performed as follows: 10 μl of the enzyme solution was added to the 2 mM $_{L}$ leucine paranitroanilide. (Leu-*p*NA) in 12.5 mM Mes/NaOH buffer (pH 6.4) which contain 10% (v/v) DMSO. Enzyme reaction was carried out at 37 °C for 1 to 5 min. The increase in absorbance at 405 nm attributable to release of *p*-nitroaniline was monitored continuously using a microplate reader (SH-8000 Lab; CORONA ELECTRIC Co.,Ltd.). The initial rates of the hydrolytic activity were determined from the linear portion of the optical density profile.

The optimum pH of enzyme activities was tested in a four-component buffer, which consisted of 5 mM glycine, 5 mM acetic acid, 5 mM Mes, and 15 mM Tris. The buffer was titrated to the desired pH with HCl or NaOH. In the assays, Leu-*p*NA at 100 μM was used as substrate. Thermal stability testing was carried out as follows: the enzyme solutions were incubated at various temperatures (20–75°C) for 30 min at pH 6.4. Then, their residual activity toward Leu-pNA were measured. The substrate specificity toward *p*NA derivative of amino acids were tested at pH 6.4 and at pH 7.5 in the above fore-component buffer system. The kinetic parameters (K_{cat} and K_m) against Leu-pNA was determined by the Lineweaver-Burk plot.

The hydrolytic activity toward puromycin was evaluated by the LC/UV method described as follows. The reaction mixture (50 μL) was composed of 12.5 mM Mes/NaOH buffer (pH 6.4), 2.0 mM puromycin, and 4.7 μg of purified ACAP. The enzyme reaction was conducted at 37 °C for 60 min followed by the addition of 100 μL of 3% (v/v) HCOOH for quenching the reaction. The solution was centrifuged and 10 μl of the supernatant was applied to ODS-HPLC analysis monitored at UV 270 nm. The mobile phase was water containing 0.1 % (v/v) HCOOH (A) and MeOH containing 0.1 % (v/v) HCOOH (B) at a flow rate of 0.2 mL/ min. The LC condition was 15% B during 0–5 min and a linear increase from 15–60 % B during 5–30 min. Under these conditions, the PM substrate and its hydrolyzed product PAN were eluted at 22.6 min and 5.1 min, respectively.

TableS2. Biochemical properties of ACAP

Properties		Supporting information
Molecular mass (kDa)	69.8	
Catalytic Ser	Ser^{491}	
Optimum pH	6.4	Figure S1
Thermal stability (°C)	< 65[1)]	Figure S2
Optimum temperature	65	Figure S3
Inhibitor[2)]	PMSF	
Hydrolytic activity (μmol/min/mg)		
Substrates		
Leu-*p*NA (2.0 mM) [3)]	105 (±0.65)	Figure S4
Phe-*p*NA (1.0 mM) [3)]	57.1 (±0.01)	Figure S4
Met-*p*NA (2.0 mM) [3)]	44.2 (±1.18)	Figure S4
Pro-*p*NA (2.0 mM) [3)]	9.55 (±0.09)	Figure S4
Phe-NH_2 (5.0 mM) [4)]	23.9 (±1.15)	
Phe-Phe-NH_2 (5.0 mM)[4)]	18.7 (±0.96)	
Phe-Phe (5.0 mM)[4)]	16.0 (±1.47)	
Phe-Ala (5.0 mM) [4)]	2.85 (±0.19)	
Leu-Phe (5.0 mM) [4)]	2.30 (±0.87)	
Phe-OMe (10.0 mM) [4)]	30.7 (±2.18)	
Puromycin (2.0 mM) [5)]	0.124 (±0.01)	
K_m(mM)[6)]	0.693 (±0.05)	Figure S5
K_{cat}(s^{-1})[6)]	154 (±1.90)	Figure S5

1) Approximately 80% of enzyme activity remained after heat treatment at 65 °C for 30 min. In addition, as shown in Figure S2, activity-enhancement was observed by heat treatment at around 60 °C for 30 min. For this experiment, Leu-*p*NA was used as substrate. 2) 100 μl (0.1 mg/ml) of enzyme solution was treated with 2.0 mM phenylmethylsulfonyl fluoride (PMSF) at 30 °C for 30 min, after which the residual activity toward 2mM Leu-*p*NA was measured. The residual activity was 47.3%. 3) At pH 6.4 in 12.5 mM Mes/NaOH buffer containing 10 % (v/v) DMSO. 4) At pH 5.5 in 80 mM AcOH/NaOH buffer. 5) At pH 6.4 in 12.5 mM Mes/NaOH buffer without DMSO. 6) Toward Leu-*p*NA at pH 6.4 in 12.5 mM Mes/NaOH buffer.

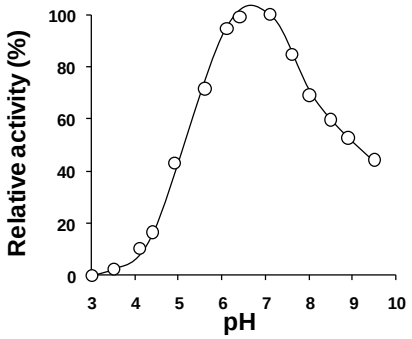

Figure S1. Optimum pH of ACAP for Leu-*p*NA hydrolysis

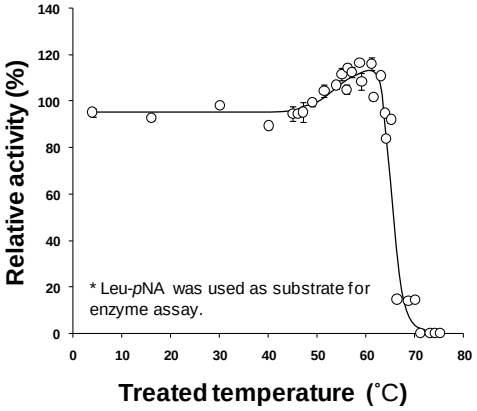

Figure S2. Thermal stability of ACAP

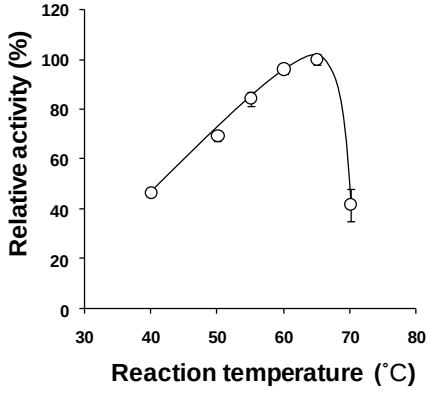

Figure S3. Optimum temperature of ACAP for Leu-*p*NA hydrolysis

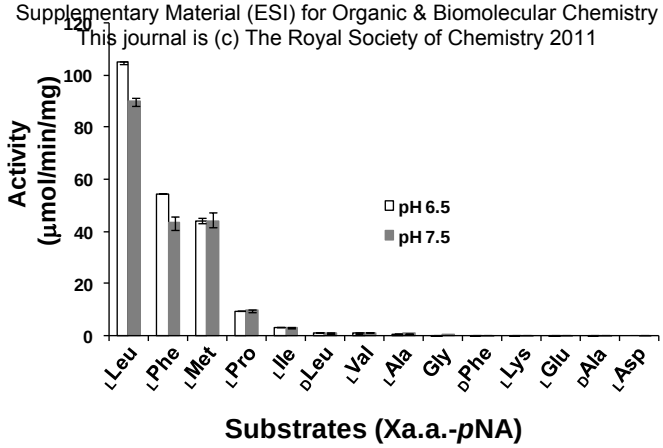

Figure S4. Aminopeptidase activity of ACAP toward *p*NA derivatives of amino acids.

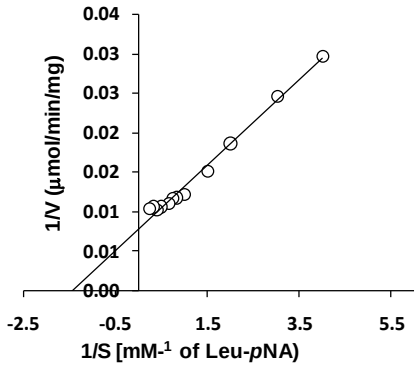

Figure S5. Linweaver burk plot

Section-3: MS spectra of synthesized homo-peptides shown in Figure 2 of the main text.

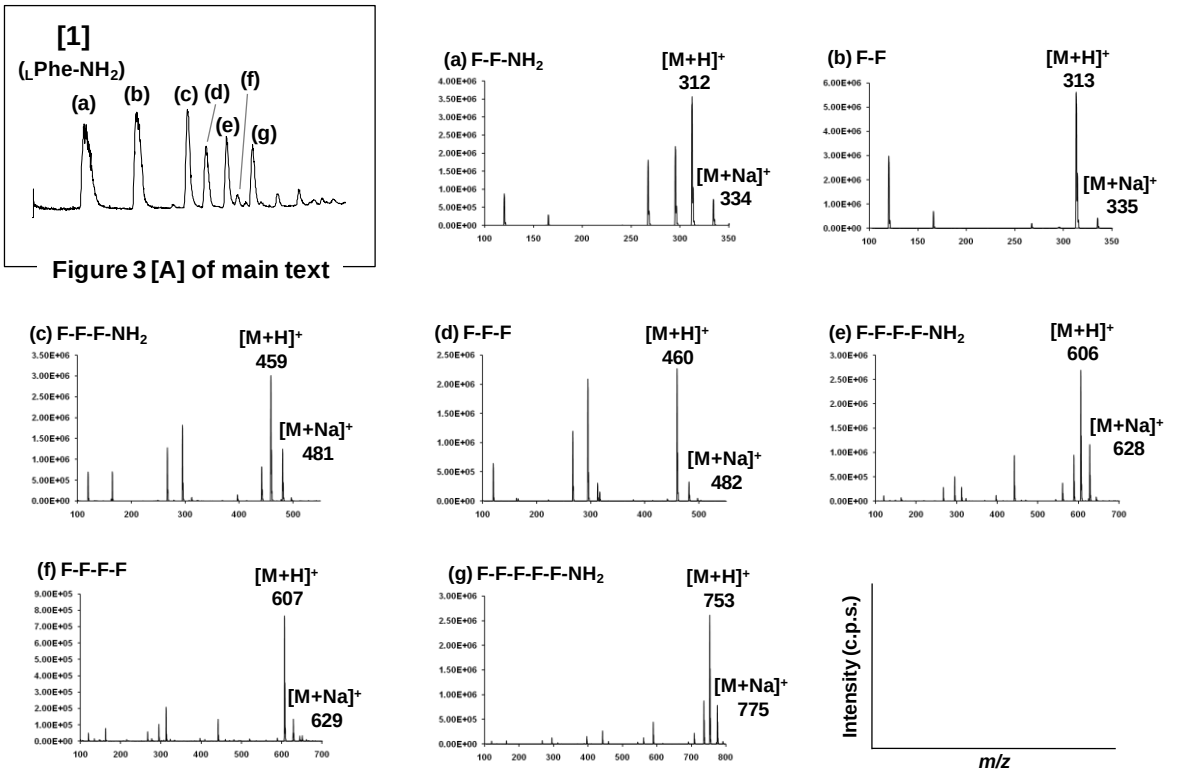

Figure S6-1. MS spectra of produced homo-peptides shown in Figure 3 [A] of main text.

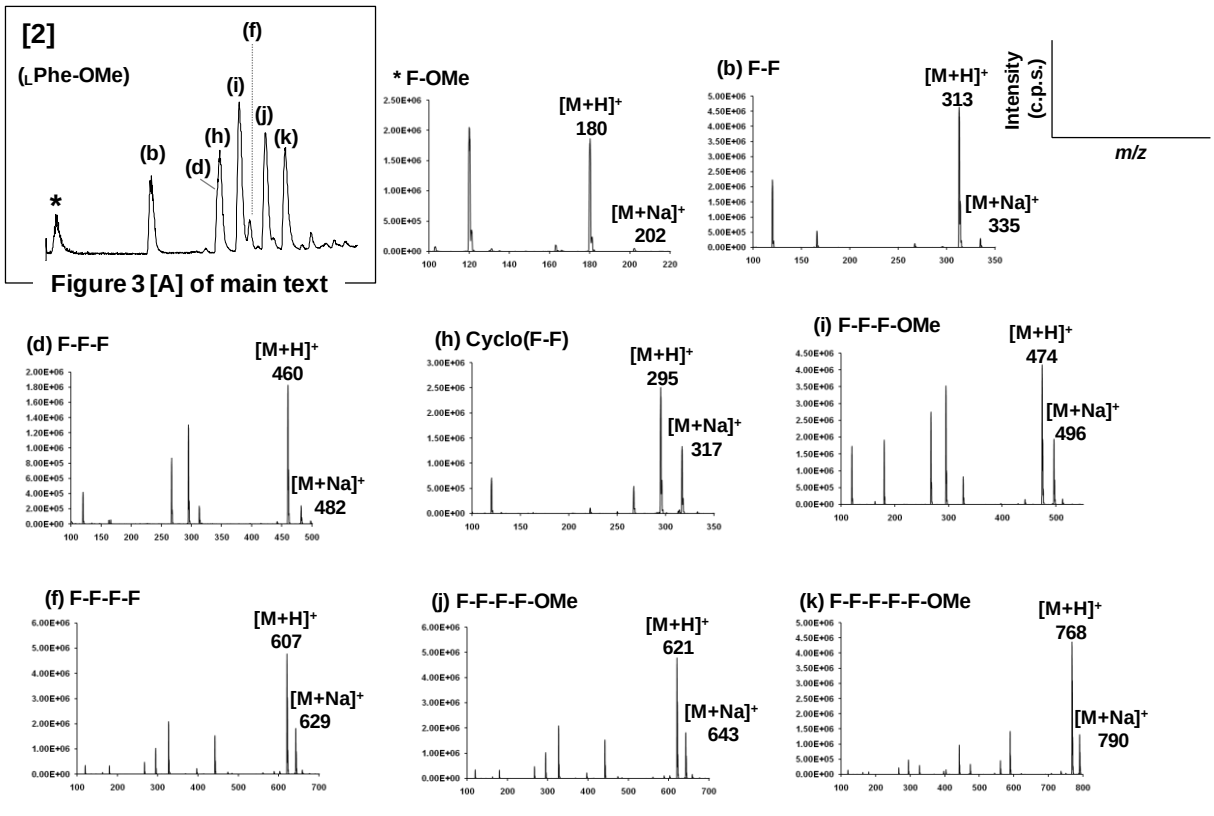

Figure S6-2. MS spectra of produced homo-peptides shown in Figure 3 [A] of main text.

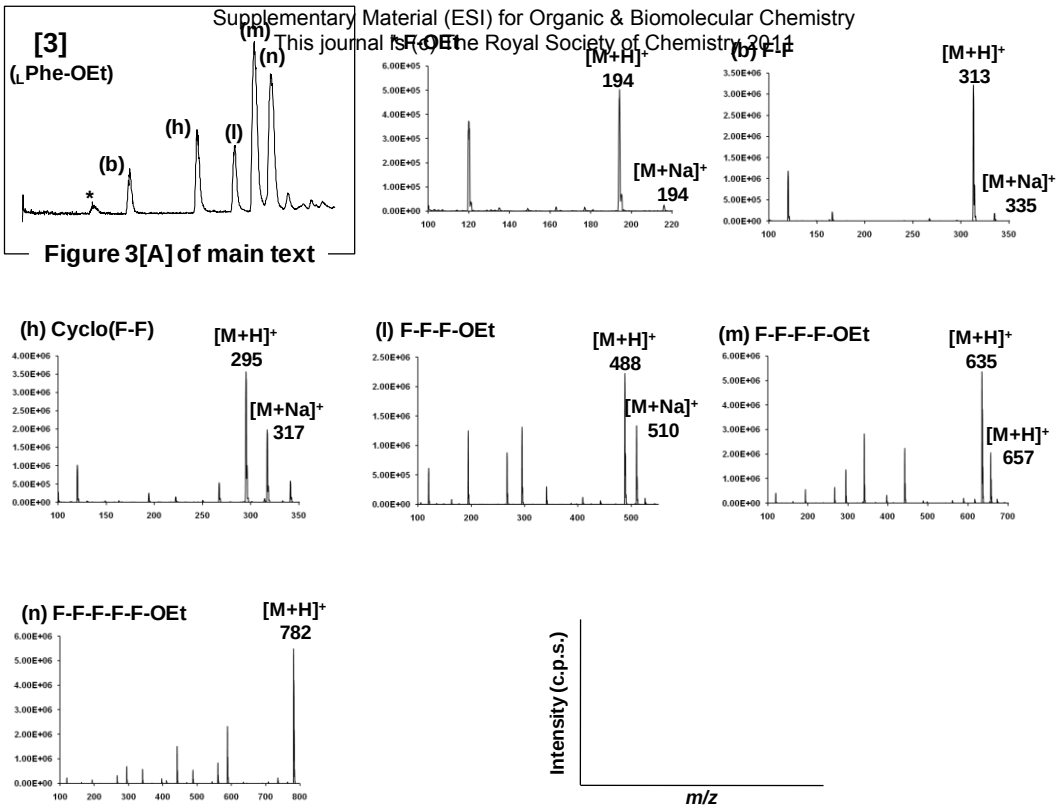

Figure S6-3. MS spectra of produced homo-peptides shown in Figure 3[A] of main text.

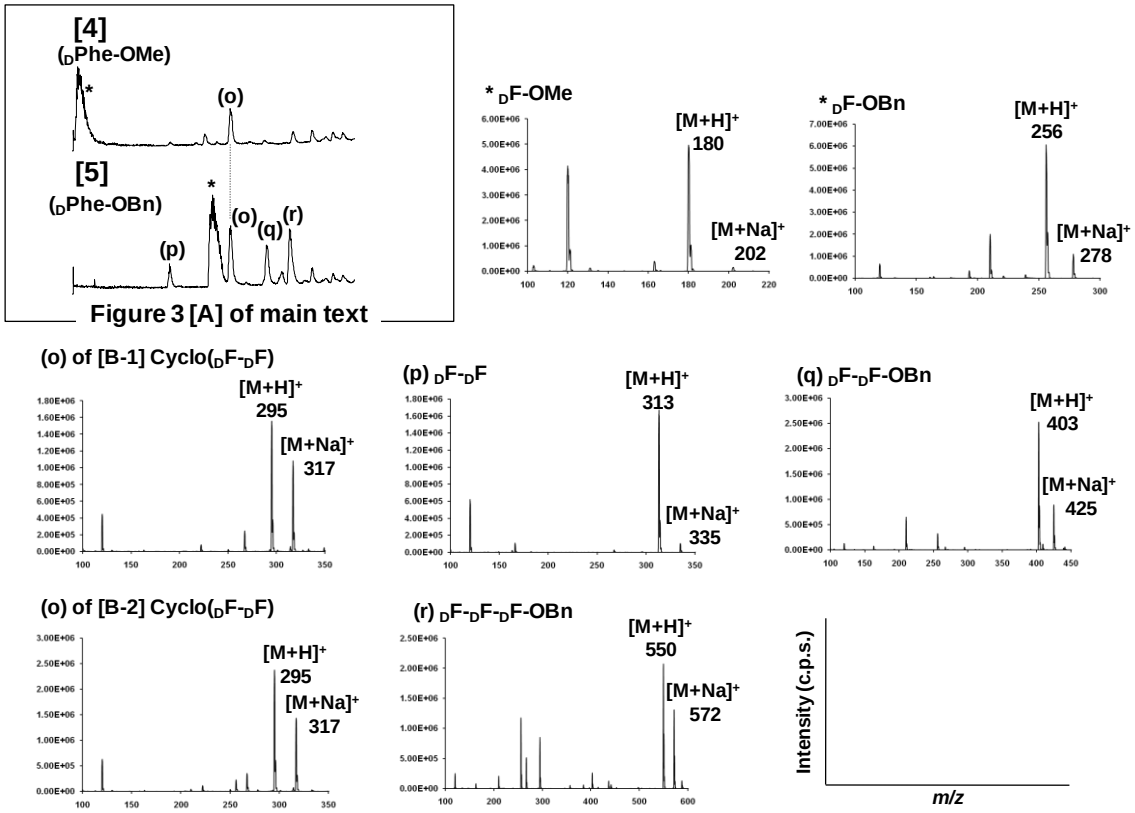

Figure S6-4. MS spectra of produced homo-peptides shown in Figure 3 [A] of main text.

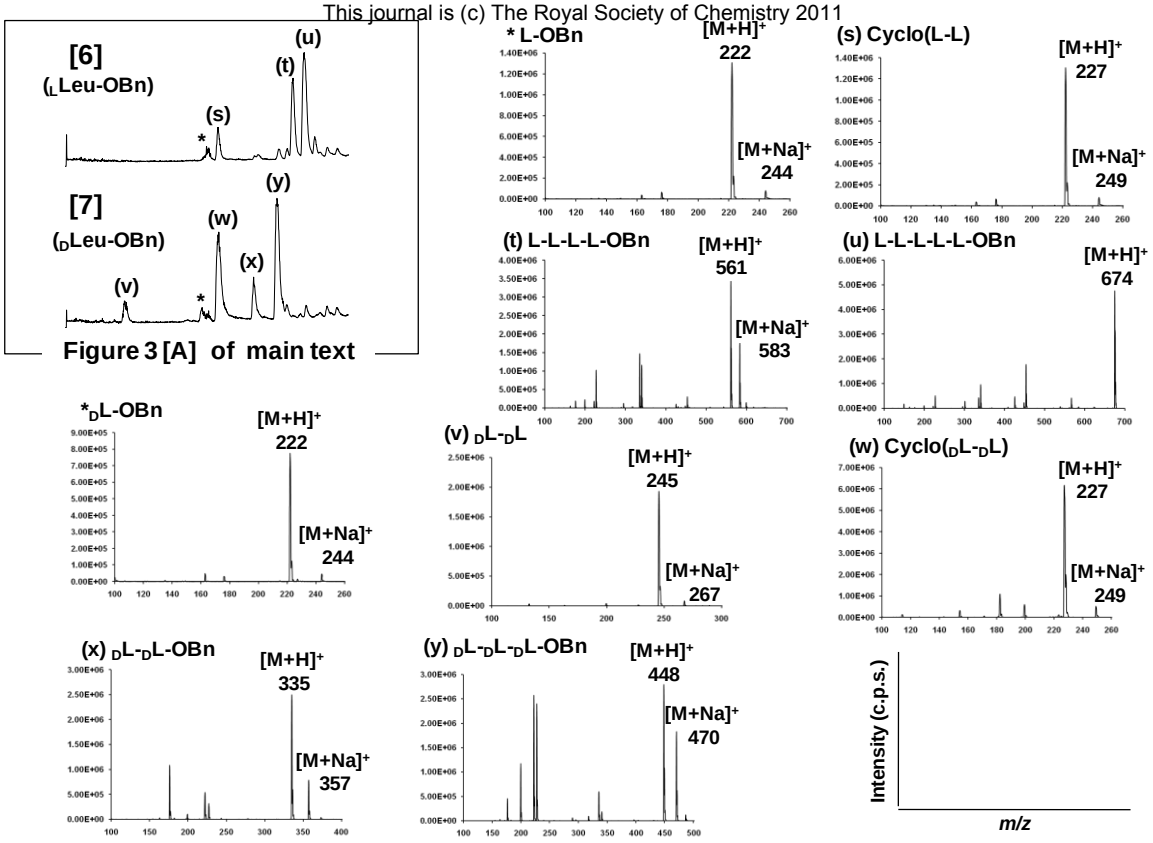

Figure S6-5. MS spectra of produced homopeptides shown in Figure 3 [A] of main text.

Section-4. Homo-peptide synthesis

The procedure of the enzyme reaction was described in the Experimental Section of the main text. The C-terminal modified amino acids listed in Table S3 were subjected to the reaction. The underlined compounds were recognized by aminolysin-*A*. The total ion chromatograms (TICs) of the reaction mixtures and MS spectra of products, obtained by the use of $_{L}$-Phe-NH_2, $_{L}$-Phe-OMe, $_{L}$-Phe-OEt, $_{D}$-Phe-OMe, $_{D}$-Phe-OBn, $_{L}$-Leu-OBn, and $_{D}$-Leu-OBn, were already shown in the Figure 3[A] of the main text and Figure S6s as typical examples of these experiments. Product identification for the others (underlined compounds in Table S3) is summarized in Table S4.

Table S3. **List of tested amino acid derivatives for homo-peptide synthesis**

A mino acid moieties	Types of derivatization of carboxyl group	Companies	Amino acid moieties	Types of derivatization of carboxyl group	Companies
L-Lys	OMe	SIGMA	L-Ala	NH_2	novabiochem
	OBzl	BACHEM		OMe	ALDRICH
L-Arg	OMe	BACHEM		OBzl	Tokyo Chemical Industry
L-His	OMe	ALDRICH	D-Ala	NH2	BACHEM
L-Ile	OBzl	BACHEM		OMe	BACHEM
L-Phe	NH_2	novabiochem		OBzl	BACHEM
	OMe	ALDRICH		Ot-butyl	BACHEM
	OEt	ALDRICH	L-Met	OMe	SIGMA
D-Phe	OMe	ALDRICH	L-Pro	OMe	ALDRICH
	OBzl	BACHEM		OBzl	BACHEM
L-Leu	NH2	novabiochem	D-Pro	OBzl	BACHEM
	OMe	ALDRICH	L-Asp	$O(Me)_2$	ALDRICH
	OEt	BACHEM		OBzl	BACHEM
	OBzl	PEPTIDE INSTITUE	D-Asp	OBzl	BACHEM
	Ot-butyl	SIGMA	L-Glu	$O(Et)_2$	ALDRICH
	Oallyl	SIGMA		OBzl	BACHEM
D-Leu	OBzl	BACHEM	D-Glu	OBzl	BACHEM
L-Ile	OBzl	BACHEM	L-Thr	OMe	SIGMA
D-Ile	OBzl	BACHEM		OBzl	novabiochem
L-Trp	OBzl	BACHEM	D-Thr	OBzl	BACHEM
	OMe	ALDRICH	L-Gln	NH2	BACHEM
D-Trp	OBzl	BACHEM	D-Gln	NH2	BACHEM
L-Cys	OMe	ALDRICH	L-Tyr	NH2	novabiochem
L-Asn	OMe	BACHEM		OMe	ALDRICH
L-Val	OMe	ALDRICH		OBzl	BACHEM
	OBzl	BACHEM	D-Tyr	OBzl	BACHEM
D-Val	OBzl	BACHEM	Gly	OMe	ALDRICH
				OBzl	SIGMA
			L-Ser	OMe	ALDRICH
				OBzl	BACHEM
			D-Ser	OBzl	BACHEM

*The underlined compounds were recognized by aminolysin-*A*.

Table S4. C-terminal modified amino acids recognized by aminolysis-A

Substrates	Poducts[1)]	Retention time (min.)	Observed *m/z*, $[M+H]^+$
$_L$-Ile-OBn	Cyclo (Ile-Ile)	25.8	227.2
	Ile-Ile-OBn	33.6	335.3
	Ile-Ile-Ile-OBn	37.8	448.2
$_L$-Leu-OMe	Cyclo (Leu-Leu)	26.6	227.2
$_L$-Leu-OEt	Cyclo (Leu -Leu)	26.6	227.2
$_L$-Leu-NH_2	Leu-Leu-Leu-NH_2	23.3	357.2
	Cyclo (Leu -Leu)	26.6	227.2
$_L$-Trp-OMe	Trp-Trp	25.3	391.2
	Cyclo (Trp-Trp)	26.8	373.1
	Trp-Trp-Trp	30.4	577.2
	Trp-Trp-Trp-OMe	34.0	591.2
$_L$-Trp-OBn	Cyclo (Trp-Trp)	26.8	373.1
$_D$-Trp-OBn	Cyclo ($_D$Trp-$_D$Trp)	26.8	373.1
$_L$-Met-OMe	Met-Met	9.4	281.1
	Cyclo (Met-Met)	20.6	263.2
$_L$-Tyr-NH_2	Tyr-Tyr	10.0	345.2
	Cyclo (Tyr-Tyr)	14.7	327.2
	Tyr-Tyr-Tyr-NH_2	16.6	507.3
	Tyr-Tyr-Tyr	19.1	508.3
$_L$-Tyr-OBn	Cyclo (Tyr-Tyr)	14.7	327.2
	Tyr-Tyr-Tyr	19.1	508.3
$_L$-Tyr-OMe	Tyr-Tyr	10.2	345.2
	Cyclo (Tyr-Tyr)	14.9	327.1
	Tyr-Tyr-Tyr	19.1	508.3

1) Speculated compounds judged from its observed *m/z* and retention time on HPLC/MS analysis were shown.

Section-5. Confirmation of non-enzymatic cyclization of $_D$F-$_D$F-OBn to give *cyclo*($_D$F-$_D$F)

In order to clarify the reaction mechanism to give cyclic dipeptides, we tried to isolate the intermediate dipeptide ester and then subject it to enzymatic and non-enzymatic treatments. In this experiment, $_D$-F-OBn was selected as the model substrate because of its ability to give a linear dipeptide ester and cyclic dipeptide under our reaction system (see Figure S6-4). The reaction mixture (1000 μl) was composed of 0.1 M phosphate buffer (pH 8.0), 10 mM $_D$F-OBn, 100 μg purified aminolysin-*A*, and 10% (v/v) DMSO. The reaction was performed at 21 °C (room temperature) for 6 h using a Capsule HF 120 centrifuge (TOMY, Tokyo, Japan), in which three separate reactions were conducted. It should be noted that the conditions, including a low reaction temperature and centrifugation, were effective for obtaining the final product *cyclo*($_D$-F-$_D$-F) as an insoluble pellet. After the reaction, the three separate reaction mixtures were combined and centrifuged, and the upper layer containing $_D$-F-$_D$-F-OBn was subjected to preparative ODS HPLC with the gradient solvent system of MeOH/H_2O to isolate 8.7 μg of produced $_D$-F-$_D$-F-OBn. The isolate was subjected to the following treatment. The reaction mixture (100 μL) was composed of 0.1 M NaPi (pH 8.0), 50 μM of isolated $_D$-F-$_D$-F-OBn, and 10% (v/v) DMSO with or without 10 μg of aminolysin-*A*. The reaction was conducted at 50 °C for 6 h followed by the addition of 100 μL of MeOH for quenching. After centrifugation, 10 μL of the supernatant was subjected to a UPLC/MS analysis, for which the ACQUITY Ultra Performance LC® System (Waters) connected to the API 2000 LC/MS/MS System (Applied Biosystems) was used. In this experiment, selected ion monitoring was used for the detection of the substrate, $_D$F-$_D$F-OBn; the putative products, *cyclo*($_D$-F-$_D$-F); and the linear dipeptide, $_D$-F-$_D$-F. The column used was an ACQUITY UPLC BEH C18 (1.7 μm, 2.1 x 50 mm). The mobile phase was water containing 0.1% (v/v) HCOOH (A) and MeOH containing 0.1% (v/v) HCOOH (B) at a flow rate of 0.3 ml/min. The LC condition was 20% B during 0–2 min and a linear increase from 20% to 65% B from 2 min to 10 min, while the flow was diverted from the mass spectrometer to the waste during 0–1.5 min. The results are shown in Figure S7. Apparently, $_D$-F-$_D$-F-OBn was non-enzymatically converted to *cyclo*($_D$-F-$_D$-F). From this observation, we concluded that the cyclization (intramolecular aminolysis) of the intermediate dipeptide ester took place in a non-enzymatic manner.

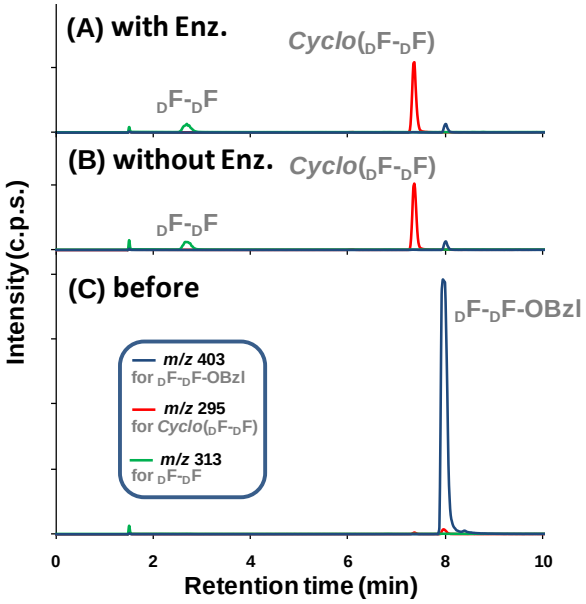

Figure S7. Non-enzymatic intramolecular aminolysis of $_D$F-$_D$F-OBn to give *cyclo* ($_D$F-$_D$F). (A) 50 μM of $_D$-F-$_D$-F-OBn was treated at 50°C for 6 h with 10 μg of aminolysin-*A*.(B) Treated without aminolysin-*A*. (C) $_D$-F-$_D$-F-OBn as substrate (before the above treatment).

Section-6: Hetero-peptide synthesis

The procedure of the enzyme reaction was described in the Experimental Section of the main text. The free amines listed in Table S5 were subjected to the reaction. The underlined compounds were recognized by aminolysin-*A* to give $_{L}$-Phe- and $_{L}$-Met-containing dipeptides. Figure S8 shown the extracted ion chromatograms (XICs) for the synthesis of $_{L}$-Met-containing dipeptides. The procedures for the construction of XICs were described in the Experimental section of the main text. LC elution programs for Figure S8 were following. The mobile phase was water containing 0.1 % (v/v) HCOOH (A) and MeOH containing 0.1 % (v/v) HCOOH (B) at a flow rate of 0.2 ml/ min. The LC condition was 5.0 % B during 0–5 min, a linear increase from 5.0–99 % B during 5–40 min, and 99% B during 40–45 min.

Table S5. List of tested free amines for hetero-peptide synthesis

Compounds	Companies	Compounds	Company
$_{L}$-Lys	WAKO	(*R*)-α-Methylphenylalanine	NAGASE and CO., LTD. (Japan)
$_{L}$-Arg	WAKO	(*S*)-α-Methylphenylalanine	NAGASE and CO., LTD. (Japan)
$_{L}$-His	WAKO	(*R*)-α-Methyl-3-nitrophenylalanine	NAGASE and CO., LTD. (Japan)
$_{D}$-His	WAKO	(*S*)-α-Methyl-3-nitrophenylalanine	NAGASE and CO., LTD. (Japan)
$_{L}$-Ile	nacalai	(*S*)-β-(4-Bisphenyl)-α-methylalanine	NAGASE and CO., LTD. (Japan)
$_{L}$-Phe	WAKO	(*S*)-4-Bromo-α-methylphenylalanine	NAGASE and CO., LTD. (Japan)
$_{D}$-Phe	BACHEM	(*S*)-4-Iodo-α-methylphenylalanine	NAGASE and CO., LTD. (Japan)
$_{L}$-Leu	WAKO	(*R*)-α-Methyltyrosine	NAGASE and CO., LTD. (Japan)
$_{D}$-Leu	ALDRICH	(*S*)-α-Methyltyrosine	NAGASE and CO., LTD. (Japan)
$_{L}$-Trp	WAKO	(*R*)-α-Allylglycine	NAGASE and CO., LTD. (Japan)
$_{D}$-Trp	SIGMA	(*S*)-α-Allylglycine	NAGASE and CO., LTD. (Japan)
$_{L}$-Ala	WAKO	(*R*)-α-Propargylglycine	NAGASE and CO., LTD. (Japan)
$_{D}$-Ala	WAKO	(*S*)-α-Propargylglycine	NAGASE and CO., LTD. (Japan)
$_{L}$-Met	WAKO	(*R*)-α-Methylleucine	NAGASE and CO., LTD. (Japan)
$_{L}$-Pro	nacalai	(*S*)-α-Methylleucine	NAGASE and CO., LTD. (Japan)
$_{L}$-Val	WAKO	Puromycin aminonucleoside	SIGMA ARDRICH
$_{L}$-Asp	WAKO		
$_{L}$-Glu	WAKO		
$_{L}$-Thr	nacalai		
$_{D}$-Thr	SIGMA		
$_{L}$-Gln	WAKO		
$_{D}$-Gln	SIGMA		
$_{L}$-Tyr	WAKO		
$_{D}$-Tyr	ALDRICH		
Gly	WAKO		
$_{L}$-Ser	WAKO		
$_{L}$-Cys	SIGMA		
$_{D}$-Cys	WAKO		
$_{L}$-Asn	WAKO		
$_{D}$-Asn	WAKO		
$_{D}$-alpha-Ala	WAKO		

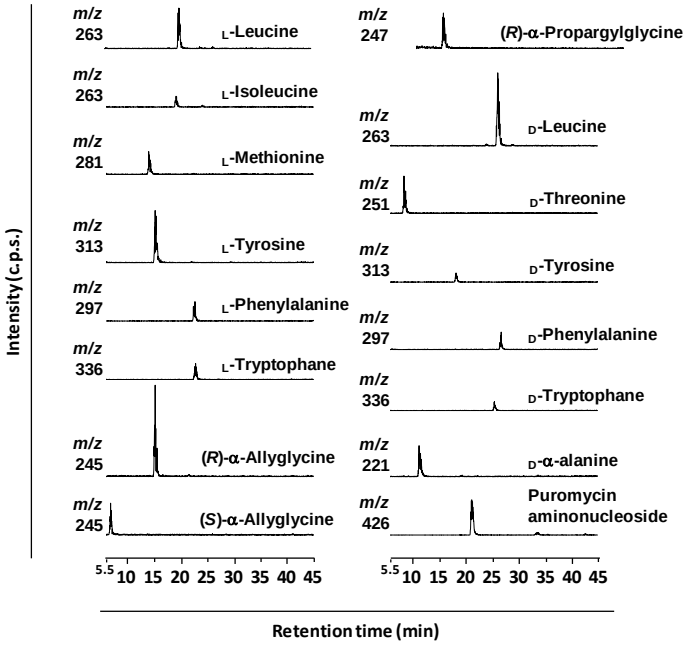

Figure S8. Methionine-containing dipeptide synthesis

Section-7. Puromycin analogue synthesis

7-1: MSMS analysis of synthesized puromycin analogues (X-PANs) and authentic puromycin (Figure 4 of the main text)

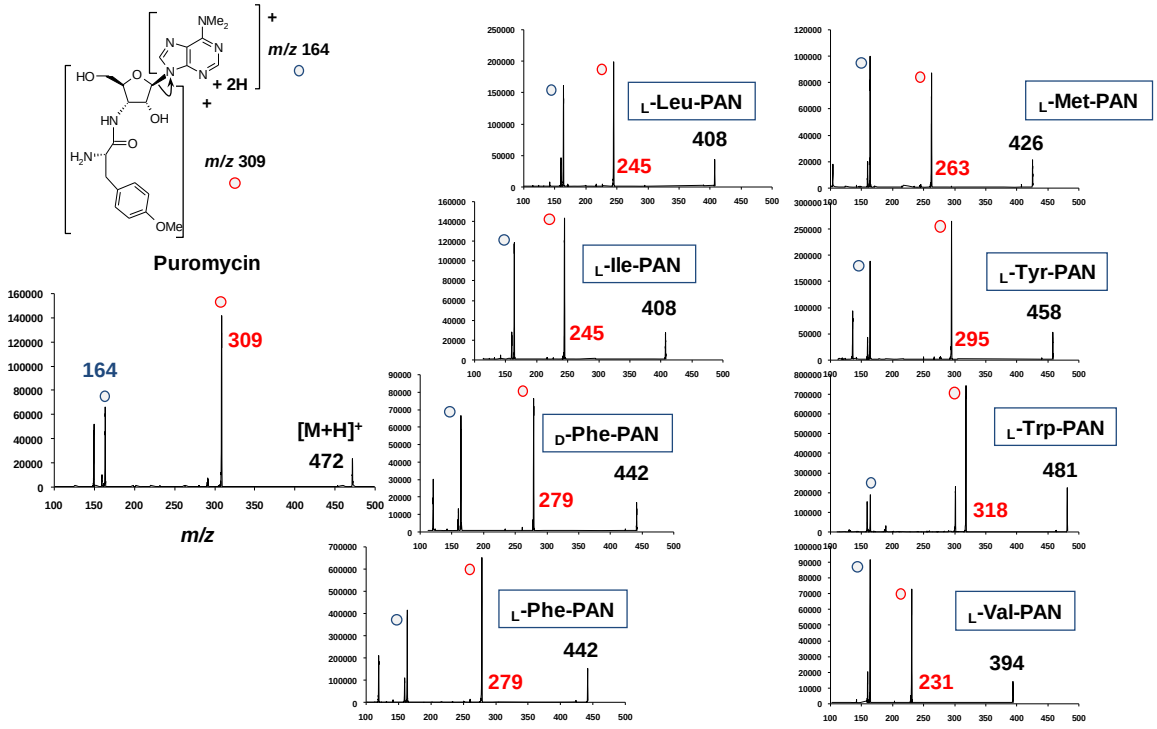

Figure S9. MS/MS spectra of puromycin and synthesized puromycin analogues (X-PANs) corresponding to Figure 4[A] of the main text

7-2. MRM quantification of synthesized puromycin analogues (X-PANs) as a substitute for authentic puromycin (Table 1, 2, and figure 4,5 of main text)

The MS/MS spectrum of the authentic puromycin was shown in Figure S9. As shown, 2 ions corresponding to *m/z* 309 and *m/z* 164 were characteristic fragmentation ions of puromycin skeleton. Therefore, we created the 2 kinds of MRM transition sets, in those the experimental parameters were optimized using authentic puromycin. The MRM transitions (Q1>Q3) for each compounds was shown in the main text. For the quantification of each X-PAN as substitute for puromycin, MRM transition set as "*m/z* of precursor ions" > "*m/z* of fragmentation ions corresponding to *m/z* 309 from puromycin" was used (see Figure S9).